Magnetic Interaction in Dinuclear Triphos−Cobalt Complexes with Co···Co Separations of 8 and 10 Å

Katja Heinze, Gottfried Huttner*, and Peter Schober

University of Heidelberg, Department of Inorganic Chemistry,
Im Neuenheimer Feld 270, D-69120 Heidelberg, Germany
Fax: (internat.) +49(0)6221/545707
E-mail: katja@sun0.urz.uni-heidelberg.de

Received September 23, 1997

Keywords: Tripodal ligands / Cobalt complexes / Bridging ligands / Exchange coupling

Weak antiferromagnetic exchange interactions are observed in two Co^{II} dimers of the general formula $[\{(triphos)Co\}_2(\mu\text{-dicarboxylato})](BF_4)_2$ where the dicarboxylate is the dianion of fumaric acid [**3**·$(BF_4)_2$] or terephthalic acid [**4**·$(BF_4)_2$] and triphos is the tridentate phosphorus ligand 1,1,1-tris(diphenylphosphanomethyl)ethane. In these complexes the metal ions are separated by 8 and 10 Å, as determined by X-ray crystallography. Insight into the interaction pathway is gained through molecular orbital calculations performed on model compounds. The influence of bridging-ligand distortions and the stereochemistry around the two cobalt centres is discussed.

Introduction

Magnetic exchange interactions between two paramagnetic centres have attracted considerable interest from inorganic chemists.[1][2][3] The investigations have mainly been focused on the simplest case where two electrons at two d^9-Cu^{II} centres ($S_1 = S_2 = \frac{1}{2}$) are separated by an organic spacer leading to new good quantum numbers of $S = 0$ (singlet state) and $S = 1$ (triplet state) for these systems.[1][2][3] Factors that govern the nature of the interaction such as orbital topology and orbital overlap are quite well understood and are used to design antiferro- and ferromagnetically coupled systems[4][5] although it is not yet possible to use theory to make quantitative explanations and predictions.[2] In the case of two interacting spins at two copper centres the interaction is mediated through the σ-framework of the bridging unit.[2] Maximum overlap between the bridging-ligand orbitals and the copper orbitals which leads to a stabilisation of the singlet state is obtained for a $d_{x^2-y^2}$ ground state of the copper ion in a square-planar or square-pyramidal geometry as opposed to a trigonal-bipyramidal situation.[2][7] With this favourable electronic configuration, antiferromagnetic exchange interaction is observed even with Cu···Cu separations larger than 10 Å.[6][7][13] The organic spacers employed for obtaining large intramolecular distances are dicarboxylic acids (or the dianions derived from them) with a rigid, usually conjugated, core. However, the coordination mode of carboxylates at metal centres can vary drastically (Scheme 1) and has a large influence on both the coordination geometry around the metal and the magnetic exchange interaction. A relatively large interaction is found if the carboxylate coordinates in a monodentate fashion with an additional hydrogen-bridge system (Scheme 1, iii);[6][7] an interaction is also predicted for the symmetrical bidentate coordination mode (Scheme 1, iv).[8] In other cases the magnetic interaction is small and may instead be *inter*molecular in nature.[8][9][10][11][12] One exception is the complex $[\{(bpy)(H_2O)Cu\}_2(\mu\text{-terephthalato})](ClO_4)_2$, although its structure has not so far been determined.[13]

Scheme 1. Binding modes of carboxylates R−COO^- at metal centres

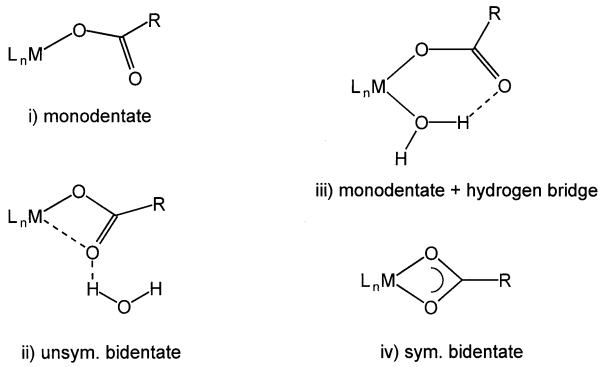

We have focused our attention on a cobalt(II) system with the tridentate ligand triphos [1,1,1-tris(diphenylphosphanomethyl)ethane]. This ligand induces a fivefold coordination around the cobalt centre providing two free *cis*-coordination sites[14][15][16] needed for a bidentate coordination mode of the carboxylate (Scheme 1, iv). The phosphorus donor set usually splits the metal-d orbitals such that a low-spin configuration (d^7) with one unpaired electron is obtained.[14][15] Furthermore the three bulky diphenylphosphano groups insulate the individual complex molecules from each other leaving no *inter*molecular interaction pathway accessible. This often represents a severe problem in the study of *intra*molecular interactions especially over large distances.[2][6]

  1434−1948/98/0202−0183 $ 17.50+.50/0

In order to address the questions concerning magnetic exchange interactions (i) within a d^7/d^7 system and (ii) over distances up to 10 Å we describe here the syntheses, solid-state structures and magnetic behaviour of dinuclear triphos−Co^{II} complexes bridged by the dianions of fumaric and terephthalic acid. In addition, we describe molecular orbital calculations which qualitatively explain the interaction pathway.

Results and Discussion

Preparation of Complexes: The reaction of triphos with $Co(BF_4)_2 \cdot 6\ H_2O$ and the appropriate dicarboxylic acid in THF/ethanol in the ratio 1:1:0.5 yields red-brown solutions from which the complex salts [{(triphos)Co}$_2$(μ-fumarato)]$(BF_4)_2$ [**3**$\cdot(BF_4)_2$] and [{(triphos)Co}$_2$(μ-terephthalato)]$(BF_4)_2$ [**4**$\cdot(BF_4)_2$] were isolated (Scheme 2).

Scheme 2. Dinuclear triphos−Co^{II} complexes

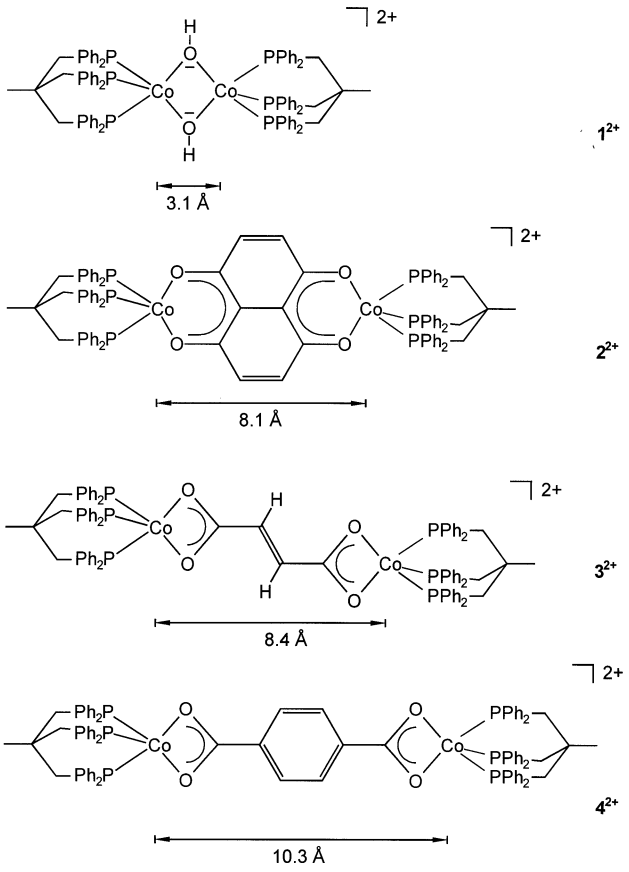

The UV/Vis spectra of the solutions are almost identical and are similar to that of the mononuclear complex [{(triphos)Co}(η^2-acetate)](BPh_4),[17] suggesting an analogous coordination environment and geometry. The absorptions observed can be assigned to d-d transitions of a square-pyramidal d^7-low-spin complex.[18][19] The dinuclear composition of $\mathbf{3}^{2+}$ and $\mathbf{4}^{2+}$ is confirmed by the observed M^+ peaks in the FAB mass spectra with correct isotopic distributions as well as signals for dications M^{2+} at *m*/2*e*. The IR spectra show the typical bands for the triphos ligand,[20] as well as the broad absorption of the tetrafluoroborate counter ions at 1055−1059 cm^{-1}. Unfortunately the $\tilde{\nu}_{as}(CO_2^-)$ and $\tilde{\nu}_s(CO_2^-)$ absorptions could not be identified as they overlap with the $\tilde{\nu}$(C=C) and δ(C−H) absorptions of the aromatic rings of the triphos ligand. For **4**$\cdot(BF_4)_2$ a medium strong band is observed at 1514 cm^{-1} which is tentatively assigned to the $\tilde{\nu}$(C=C) vibration of the aromatic ring of the bridging terephthalato ligand. In the cyclic voltammogram (CH_3CN, vs. SCE) both complexes show only quasi- and irreversible oxidation and reduction waves (see Experimental Section).

Crystal Structures: The complexes **3**$\cdot(BF_4)_2$ and **4**$\cdot(BF_4)_2$ crystallise in the monoclinic, centrosymmetric space groups $P2_1/c$ and $P2_1/n$, respectively. Table 1 summarises selected bond lengths and angles. The crystal structures consist of centrosymmetric discrete dinuclear dications (Figures 1 and 2), BF_4^- counterions and solvent molecules.

Figure 1. View of the dication of **3**$\cdot(BF_4)_2$

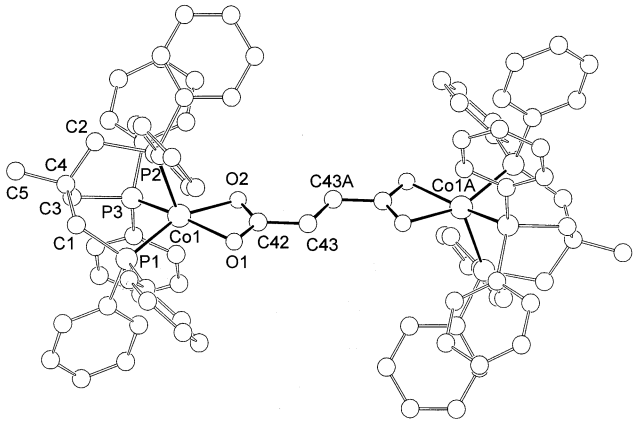

Figure 2. View of the dication of **4**$\cdot(BF_4)_2$

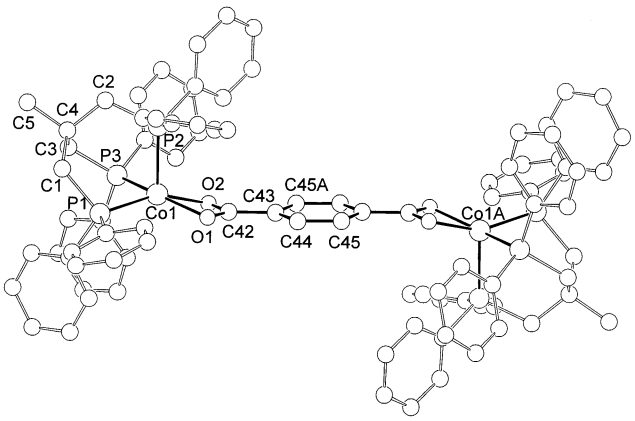

The packing of the molecules is such that no short intermolecular contacts arise: Co···Co(intermolecular) 11.8 Å [**3**···$(BF_4)_2$], 11.6 Å [**4**···$(BF_4)_2$], Co···F 7.6−10 Å [**3**···$(BF_4)_2$], 9−11 Å [**4**···$(BF_4)_2$] which provide perfect magnetic insulation of the dimeric cations. The geometry around the metal centres can be described as distorted square-pyramidal with the P2 atom occupying the axial coordination site (Figures 1 and 2). The carboxylates coordinate in a symmetric bidentate fashion with almost equal

Table 1. Selected bond lengths [Å][a] and angles [°][a] for $\mathbf{3}\cdot(BF_4)_2$ and $\mathbf{4}\cdot(BF_4)_2$

	$\mathbf{3}\cdot(BF_4)_2$	$\mathbf{4}\cdot(BF_4)_2$		$\mathbf{3}\cdot(BF_4)_2$	$\mathbf{4}\cdot(BF_4)_2$
Co1−O1	2.005(3)	2.025(4)	O1−Co1−O2	65.8(1)	66.0(2)
Co1−O2	1.998(3)	1.992(4)	P1−Co1−P2	92.15(4)	84.11(7)
Co1−P1	2.189(1)	2.204(2)	P1−Co1−P3	89.52(4)	88.96(7)
Co1−P2	2.298(1)	2.269(2)	P2−Co1−P3	90.04(4)	91.71(7)
Co1−P3	2.187(1)	2.164(2)	P1−Co1−O1	99.43(9)	106.8(2)
O1−C42	1.272(5)	1.265(8)	P1−Co1−O2	158.12(9)	155.9(1)
O2−C42	1.265(5)	1.280(7)	P2−Co1−O1	108.0(1)	98.2(1)
C42−C43	1.476(5)	1.490(8)	P2−Co1−O2	107.49(9)	109.5(1)
C43−C44	−	1.402(9)	P3−Co1−O1	159.4(1)	160.6(1)
C44−C45	−	1.395(9)	P3−Co1−O2	99.77(8)	95.1(1)
C43−C45A	−	1.39(1)	Co1−O1−C42	87.8(2)	86.5(3)
C43−C43A	1.304(8)	−	Co1−O2−C42	88.3(2)	87.6(4)
Co1···C42	2.332(4)	2.322(6)	O1−C42−C43	121.1(4)	122.9(6)
Co1···Co1A	8.37	10.31	O2−C42−C43	120.8(3)	118.5(6)
			O1−C42−O2	118.1(3)	118.5(5)

[a] Estimated standard deviations of the least significant figures are given in parentheses.

Co−O and C−O bond lengths (Table 1). The small angle O−Co−O is similar to that found in monocarboxylate complexes of the triphos−Co^{II} fragment.[16][17][21] The distance between the carbon atom of the carboxylate fragment and the central -system (double bond in $\mathbf{3}^{2+}$, aromatic ring in $\mathbf{4}^{2+}$) is that of a $C(sp^2)-C(sp^2)$ single bond.[22] The carboxylate groups and the plane of the central π-systems are almost coplanar, the tilting angle being 7.8° ($\mathbf{3}^{2+}$) and 4.2° ($\mathbf{4}^{2+}$). The intramolecular Co···Co separations are 8.37 Å ($\mathbf{3}^{2+}$) and 10.31 Å ($\mathbf{4}^{2+}$).

Magnetic Susceptibility: Variable-temperature magnetic susceptibility data for the two complexes were measured in the temperature range 7−290 K using a Faraday balance (Figures 3 and 4). These data were fitted to the Bleaney−Bowers equation[2] and the result is represented by the solid lines in Figures 3 and 4.[23] From these fits the singlet−triplet splittings are estimated as $2J = -36$ cm^{-1} [$\mathbf{3}\cdots(BF_4)_2$] and -16 cm^{-1} [$\mathbf{4}\cdots(BF_4)_2$]. *Inter*molecular interactions (vide supra) can be safely excluded and the observed antiferromagnetic exchange coupling must therefore be *intra*molecular in nature. The results are compiled in Table 2 along with the results of EPR measurements. Also included are the data of two previously described dinuclear triphos-Co^{II} complexes with oxygen donor coligands, [{(triphos)Co}$_2$(μ-OH)$_2$]$(BPh_4)_2$ [$\mathbf{1}\cdots(BPh_4)_2$][17] and [{(triphos)Co}$_2$(μ-1,4,5,8-tetraoxonaphthaleno)]$(BF_4)_2$ [$\mathbf{2}\cdots BF_4)_2$][24] (Scheme 2).

The EPR spectra in solution at 295 K and in a $THF-CH_2Cl_2$ glass at 100 K show only broad unresolved signals centred at $g = 2.12$ which is a typical value for low-spin Co^{II} complexes.[24][25][26][27][28]

Molecular Orbital Calculations: To gain insight into the possible interaction pathway, molecular orbital calculations on idealised and simplified model compounds were performed at the SCF level of theory. The frontier molecular orbitals of the complexes are depicted in Figures 5 and 6. The symmetry labels *g* and *u* refer to the inversion centres of the molecules. According to Hoffmann[3] the splitting of the singlet and triplet state is related to the energy difference

Figure 3. Temperature dependence of χ_M and μ_{eff} of a solid sample of $\mathbf{3}\cdot(BF_4)_2$

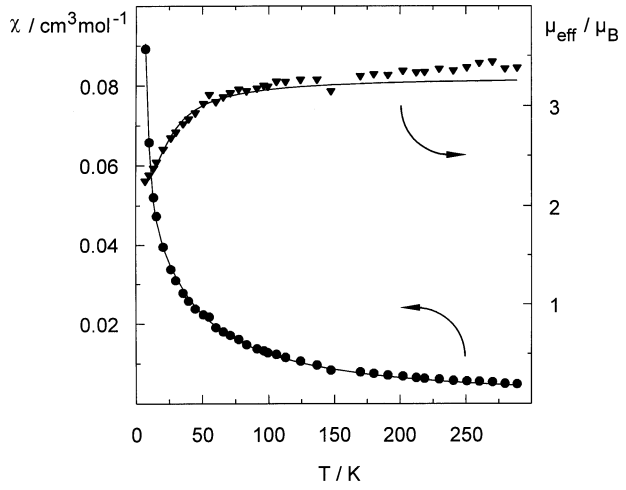

Figure 4. Temperature dependence of χ_M and μ_{eff} of a solid sample of $\mathbf{4}\cdot(BF_4)_2$

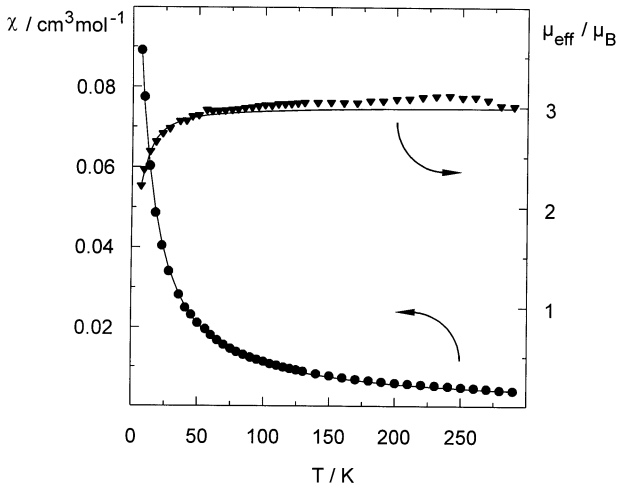

Table 2. Magnetic and EPR data of dinuclear triphos−Co^{II} complexes

compound	$-2J/cm^{-1}$	g_{mag}	g (295 K)	Ref.
$\mathbf{1}^{2+}$	144	2.45	n.d.	[17]
$\mathbf{2}^{2+}$	58	1.99	2.11	[24]
$\mathbf{3}^{2+}$	36	2.03	2.12	this paper
$\mathbf{4}^{2+}$	16	1.82	2.12	this paper

of the two frontier molecular orbitals $\varepsilon_1 - \varepsilon_2$ through $-2J = E_T - E_S = -2K_{ab} + (\varepsilon_1 - \varepsilon_2)^2\cdot(J_{aa} - J_{ab})^{-1}$ where K_{ab} is the two-electron exchange integral and J_{aa}, J_{ab} are the one- and two-centre coulomb repulsion integrals. Assuming that K_{ab}, J_{aa}, and J_{ab} vary only slowly in closely related compounds the energy difference of the *spin states* is proportional to the square of the splitting of one-electron *energy levels*.

As expected from simple ligand-field theory[29] the unpaired electron of each cobalt centre in a square-pyramidal coordination geometry occupies a d_{z^2} orbital (with an ad-

Figure 5. Orbital splitting and orbital symmetry of the model complex of $\mathbf{3}^{2+}$ [a]

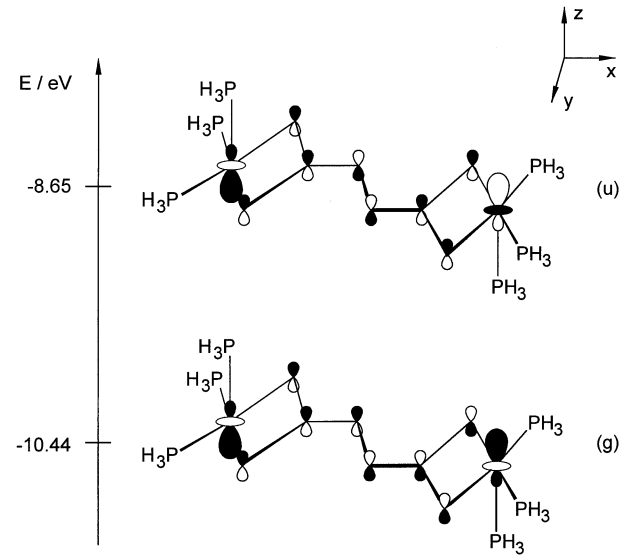

[a] The contribution of ligand orbitals is exaggerated. The composition is approximately 77% metal, 20% PH_3 and 3% bridging ligand.

Figure 6. Orbital splitting and orbital symmetry of the model complex of $\mathbf{4}^{2+}$ [a]

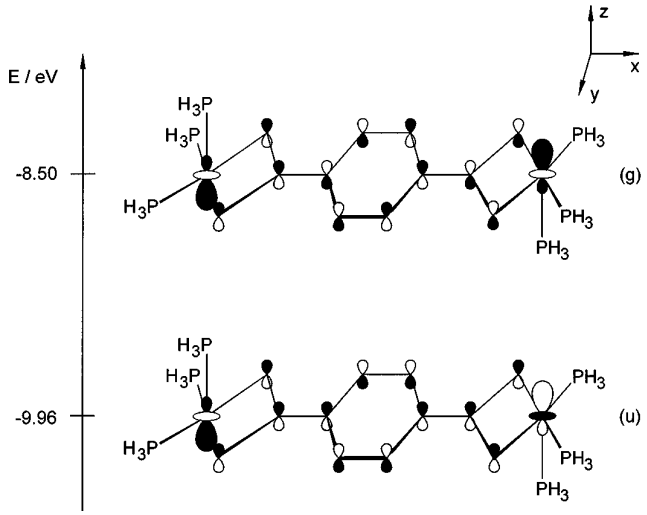

[a] The contribution of ligand orbitals is exaggerated. The composition is approximately 77% metal, 20% PH_3 and 3% bridging ligand.

mixture of 5% s and 9% p_z). The highest occupied orbitals of the dimer are the symmetric and antisymmetric combinations of these monomer orbitals. In the fumarato complex ($\mathbf{3}^{2+}$) the in-phase combination (*g*, Figure 5) is lower in energy than the out-of-phase combination (*u*, Figure 5), while the reverse is true for the terephthalato complex ($\mathbf{4}^{2+}$) (Figure 6). The qualitative level ordering of the ligand orbitals follows the expected trend from nodal structure: one (HOMO) and two (LUMO) nodal planes for the ligand-MOs of $\mathbf{3}^{2+}$ and two (HOMO) and three (LUMO) for $\mathbf{4}^{3+}$ (Figures 5 and 6).

As opposed to the d^9/d^9 case (Cu^{II}/Cu^{II}) the magnetic orbitals of the cobalt centres (d_{z^2} + p_z) are orientated almost perpendicular (*z* axis) to the plane of the carboxylato group (*xy* plane). This orientation precludes any interaction through the σ-framework of the bridging ligand but provides a pathway over the π-system of the bridge. The magnetic exchange coupling mediated by the π-system of the ligand is expected to be much smaller than an interaction through the σ-system (better orbital overlap) and the experimental results (small splitting in the cobalt case and larger splitting in the copper case) seem to support this expectation. However, inspite of the large distances between the metal centres and the poorer overlap between the metal and the ligand orbitals, a weak antiferromagnetic exchange is observed which is more than two orders of magnitude larger than the calculated singlet−triplet energy gap ($2J$ = -0.1 cm^{-1}, d_{M-M} = 10.3 Å) based on a statistical analysis.[2] Thus even switching from the σ-interaction pathway in Cu−Cu dimers to a π-interaction in Co−Co complexes does not prevent a magnetic coupling of the two metal centres separated by 10 Å.

In order to relate the singlet−triplet energy gap to the energy difference between the highest one-electron energy levels the HOMO−LUMO gaps of model compounds of $\mathbf{3}^{2+}$ and $\mathbf{4}^{2+}$ were calculated; also included in the calculation were models of the complexes $\mathbf{1}^{2+}$ and $\mathbf{2}^{2+}$.[17][24] The results are summarised in Table 3. In fact, the simple calculation reflects the correct ordering of decreasing antiferromagnetic interaction $\mathbf{1}^{2+} > \mathbf{2}^{2+} > \mathbf{3}^{2+} > \mathbf{4}^{2+}$ (Tables 2 and 3).

Table 3. Orbital energies and orbital energy splitting values

compound	ε_1/eV	ε_2/eV	$\Delta E^2=(\varepsilon_1-\varepsilon_2)^2$	Co···Co/Å
$\mathbf{1}^{2+}$	−12.232	−8.602	13.18	3.07
$\mathbf{2}^{2+}$	−10.533	−8.459	4.30	8.11
$\mathbf{3}^{2+}$	−10.438	−8.649	3.20	8.37
$\mathbf{4}^{2+}$	−9.958	−8.500	2.13	10.31

Furthermore the square of the calculated energy difference $\Delta E^2 = (\varepsilon_1 - \varepsilon_2)^2$ correlates well with the experimental singlet−triplet splitting $-2J$ ($-2J$ [cm^{-1}] = 11.0 × ΔE^2 [eV^2] + 0.61; r^2 = 0.982) (Figure 7) showing that even this simple and qualitative model can explain the observed antiferromagnetic interaction in d^7/d^7 dinuclear complexes.

Encouraged by these results the influence of distortions within the dinuclear complex on the singlet−triplet energy gap was studied. In the first study the central phenyl ring of the model complex $\mathbf{4}^{2+}$ was rotated around the x-axis (Figures 6 and 8). The dihedral angle between the plane of the phenyl ring and the basal planes of the metal-surrounding square pyramids was varied from 0 to 90°. Qualitatively the overlap between the p-orbitals at the carbon atoms C42 and C43 (Figures 2 and 8) should decrease and at the 90° distortion they should be strictly orthogonal leading to a vanishing HOMO−LUMO gap, ΔE, and thus to a zero antiferromagnetic interaction. With the employed calculation method the highest molecular orbitals become degenerate at a dihedral angle of 70°. However, too much significance should not be ascribed to the computed angle since the value is dependent on the choice of exponents for

Figure 7. Correlation of the experimental S/T gap ($2J$) and the the square of the calculated HOMO−LUMO gap (ΔE^2)

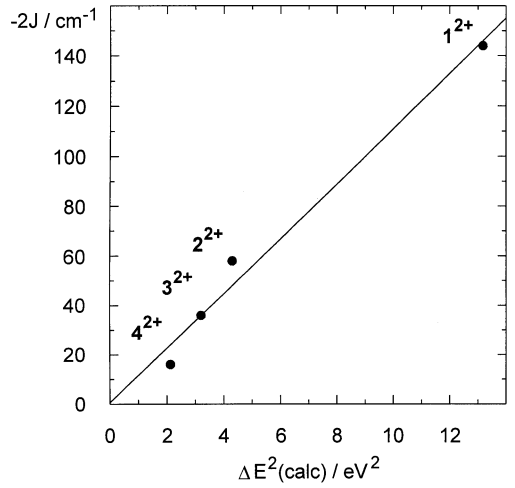

the carbon p-orbital. A similar situation was encountered in the study of the Cu−O−Cu angle variation in di-μ-OH copper dimers.[2][3] Experimentally this distortion could be achieved by attaching large substituents onto the phenyl ring of the bridging ligand; this is currently being attempted.

Figure 8. Distortion of the ligand π-system

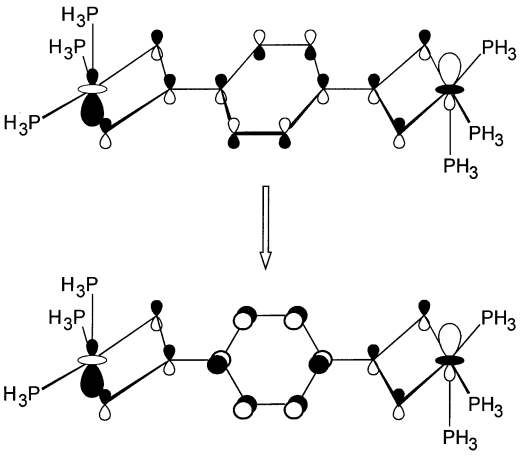

Figure 9. Square pyramid−trigonal bipyramid distortion

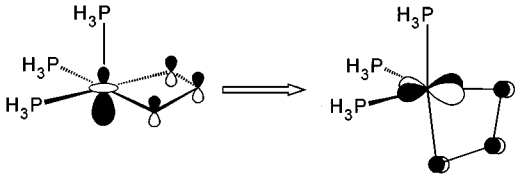

The second distortion possible in five-coordinate complexes is the transformation of the coordination polyhedron from square pyramidal to trigonal bipyramidal. This can be achieved by rotating the carboxylate chelating ligand out of the basal plane (xy plane) into the xz plane while maintaining the geometry of the $(PH_3)_3Co$ fragment (Figure 9). The hybridisation of the cobalt centres changes from d_{z^2} (+s and p_z) to almost pure d_{xy} (+p_y) (in this coordinate system) as has been shown previously.[29] The calculations show than this distortion has only a very small effect on the HOMO−LUMO energy gap; the π-type overlap of the metal d-hybrid orbitals with the oxygen p-orbitals obviously remains almost constant during the distortion. The small energy difference and activation barrier between square-pyramidal and trigonal-bipyramidal distorted triphos−Co complexes has been experimentally shown by EPR[24][25][26][27][28] and NMR spectroscopy[30][31][32] as well as by the fact that in one case both conformational isomers have been isolated in the solid state.[33] This is consistent with the assumption that neither the total energy nor the energy gap of the frontier orbitals change significantly during the distortion. Therefore unlike the Cu−Cu dimers[2][7] the singlet−triplet splitting in Co−Co dimers of the type described in this work appears relatively insensitive towards this geometrical distortion.

In summary, this work has shown that intramolecular antiferromagnetic exchange coupling occurs in dinuclear triphos−Co^{II} complexes up to a metal−metal distance of 10 Å. The interaction is transmitted through the π-system of the bridging ligand. The experimental results can be explained within a simple MO approach at the SCF level of theory. Distortions within the π-system of the bridging ligand are predicted to decrease the HOMO−LUMO gap and thus the antiferromagnetic coupling while distortions from a square-pyramidal to a trigonal-bipyramidal geometry around the metal centre are predicted to have a negligible influence on the HOMO−LUMO gap.

This work received support from the *Deutsche Forschungsgemeinschaft*, the *Fonds der Chemischen Industrie*, and the *Volkswagenstiftung*.

Experimental Section

Computational Details: Calculations were performed on an Apple Macintosh IIfx with the CACHe/ZINDO program Version 3.6 (M. C. Zerner 1990−1994) with INDO/1 parameters. Orbital energies were obtained from an SCF calculation of the singlet state without symmetry constraints. The geometry of the molecules was idealized to a square pyramidal polyhedron around the metal centre and a planar bridging ligand. The triphos ligand was replaced by three isoelectronic PH_3 groups. Distances and angles were as follows: Co−P_{eq} 2.19 Å, Co−P_{ax} 2.26 Å, Co−O 2.00 Å, P−H 1.38 Å, O−Co−O 65.8°, P−Co−P 90.0°, O−C−O 118.0°.

General Methods: Unless noted otherwise all manipulations were carried out under an inert atmosphere by means of standard Schlenk techniques. All solvents were dried by standard methods and distilled under inert gas. − NMR: Bruker AC 200 at 200.13 MHz (^{1}H). − IR: Bruker FTIR IFS-66, as CsI disks. − UV/Vis/NIR: Perkin Elmer Lambda 19. − MS: Finnigan MAT 8230. − EPR: Bruker ESP 300 E, X-band, standard cavity ER 4102, temperature control unit Eurotherm B-VT 2000, external standard diphenylpicrylhydrazyl (DPPH). − Elemental analyses: microanalytical laboratory of the Organisch-Chemisches Institut, University of Heidelberg. − Melting points: Gallenkamp MFB-595 010, melting points are not corrected. − Cyclic voltammetry: Metrohm "Universal Meß- und Titriergefäß", Metrohm GC electrode RDE 628, platinum electrode, SCE electrode, Princeton Applied Re-

search potentiostat Model 273, 10^{-3} M in 0.1 M nBu$_4$NPF$_6$/CH$_3$CN. – Magnetic measurements were carried out on a Faraday type magnetometer in the temperature range 7–290 K. The magnetic field applied was 10 kG. Mercury tetrakis(thiocyanato)cobaltate was used as a susceptibility standard. Corrections for diamagnetism were estimated using Pascal's constants[34] as $915 \cdot 10^{-6}$ [**3**·(BF$_4$)$_2$] and $955 \cdot 10^{-6}$ cm^3 mol^{-1} [**4**·(BF$_4$)$_2$]. Magnetism of the samples was found to be field-independent. The effective magnetic moment was calculated by using the equation $\mu_{eff} = 2.83\ (\chi_M\ T)^{1/2}$, whereas the exchange parameters J and g_{mag} were obtained by a least-squares fitting of the susceptibility data to the Bleaney-Bowers equation for dinuclear complexes with $S_1 = S_2 = 1/2$, where $2J$ is the energy difference between the singlet and the triplet states ($H = -2J \cdot S_1 \cdot S_2$). A further parameter p, representing the percentage of a mononuclear impurity with $S = {}^3/_2$ (high-spin Co^{II}), was introduced although the exact nature of the actual impurity (oligomer, polymer) was unknown: p = 6.7% [**3**·(BF$_4$)$_2$], 5.7% [**4**·(BF$_4$)$_2$]. The variations in g_{mag} values are not significant and result from the fitting method. Magnetic measurements in solution (CD$_2$Cl$_2$) were conducted according to the method of Evans.[35] Diphenylpicrylhydrazyl (DPPH) was used as a susceptibility standard.

Chemicals: 1,1,1-Tris(diphenylphosphanomethyl)ethane, CH$_3$C(CH$_2$PPh$_2$)$_3$[36], Co(BF$_4$)$_2$·6 H$_2$O[37].

Crystallographic Structure Determinations: The measurements were carried out on a Siemens P4 (Nicolet Syntex) R3m/v four-circle diffractometer with graphite-monochromated Mo-K_α radiation. All calculations were performed using the SHELXT PLUS software package. Structures were solved by direct methods with the SHELXS-86 program and refined with the SHELX93 program.[38] Graphics were prepared using XPMA and ZORTEP.[39] An absorption correction (ψ scan, $\Delta\psi = 10°$) was applied to all data. Atomic coordinates and anisotropic thermal parameters of the nonhydrogen atoms were refined by a full-matrix least-squares calculation. Table 4 is a compilation of the data for the structure determinations. Further details of the crystal structure determinations may be obtained from the Fachinformationszentrum Karlsruhe, D-76344 Eggenstein-Leopoldshafen (Germany), on quoting the depository numbers CSD-407616 [**3**·(BF$_4$)$_2$], and CSD-407617 [**4**·(BF$_4$)$_2$].

(μ-Fumarato)bis[{1,1,1-tris(diphenylphosphanomethyl)-ethane}cobalt] Bis(tetrafluoroborate) [**3**·(BF$_4$)$_2$] *and (μ-Terephthalato)bis[{1,1,1-tris(diphenylphosphanomethyl)ethane}-cobalt] Bis(tetrafluoroborate)* [**4**·(BF$_4$)$_2$]: A solution of Co(BF$_4$)$_2$·6 H$_2$O (341 mg, 1 mmol) in EtOH (10 ml) was added to a solution of the triphos ligand (624 mg, 1 mmol) in THF (15 ml). Addition of the dicarboxylic acid [fumaric acid for **3**·(BF$_4$)$_2$; 58 mg, 0.5 mmol; terephthalic acid for **4**·(BF$_4$)$_2$; 83 mg, 0.5 mmol] to the orange-coloured solution caused a slow colour change to red-brown. After the solution had been stirred for two hours it was filtered and the solvents were evaporated. The solid residue was washed with Et$_2$O, dissolved in CH$_2$Cl$_2$ and filtrated over 2 cm of Kieselgur. The clear, red solution was concentrated in vacuo until the complex started to precipitate. Precipitation was completed by adding 10 ml of Et$_2$O. Recrystallisation from CH$_2$Cl$_2$/Et$_2$O yielded 356 mg (43%) of **3**·(BF$_4$)$_2$ and 410 mg (48%) of **4**·(BF$_4$)$_2$, respectively. Vapour diffusion of Et$_2$O into a concentrated solution of the complex [**3**·(BF$_4$)$_2$ in acetone; **4**·BF$_4$)$_2$ in CH$_2$Cl$_2$] afforded red needle-shaped crystals suitable for X-ray crystallographic analysis.

3·(BF$_4$)$_2$: M.p. 250°C (decomp.). – IR (CsI): $\tilde{\nu}$ = 3058 cm^{-1} (m), 1485 (m), 1436 (s), 1283 (m), 1093 (s), 1055 (br), 999 (m), 829 (w), 738 (s), 692 (s), 513 (s). – MS (FAB); *m/z* (%): 1599 (18) [M$^+$ + F], 1480 (11) [M$^+$], 875 (38) [M$^+$ – triphos-Co + Ph + 1], 797 (40) [M$^+$ – triphos-Co], 740 (5) [M^{2+}], 683 (52) [triphos-Co$^+$], 547 (43) [triphos-Ph$^+$]. – UV/Vis (CH$_2$Cl$_2$): λ_{max} (ε) = 489 nm (3550 M^{-1} cm^{-1}), 966 (1030). – CV (CH$_3$CN): $E_{1/2}$ = –0.30 V (qrev.), +0.35 V (qrev.). – μ_{eff}(CD$_2$Cl$_2$): 3.5 μ_B. – C$_{86}$H$_{80}$B$_2$Co$_2$F$_8$O$_4$P$_6$ (1654.9): calcd. for **3**·(BF$_4$)$_2$·3 CH$_2$Cl$_2$: C 55.98, H 4.54; found C 55.11, H 5.04.

4·(BF$_4$)$_2$: M.p. 240°C (decomp.). – IR (CsI): $\tilde{\nu}$ = 3059 cm^{-1} (m), 1514 (m), 1485 (m), 1434 (s), 1409 (m), 1279 (w), 1096 (s), 1059 (br), 998 (m), 854 (s), 833 (w), 738 (s), 694 (s), 514 (s). – MS (FAB); *m/z* (%): 1549 (42) [M$^+$ + F], 1530 (21) [M$^+$], 925 (74) [M$^+$ – triphos-Co + Ph + 1], 847 (71) [M$^+$ – triphosCo], 765 (8) [M^{2+}], 683 (56) [triphosCo$^+$], 547 (72) [triphos-Ph$^+$]. – UV/Vis (CH$_2$Cl$_2$): λ_{max} (ε) = 474 nm (3130 M^{-1} cm^{-1}), 650 (230), 963 (880). – CV (CH$_3$CN): E_p = –0.37 V (irr.), $E_{1/2}$ = +0.27 V (qrev.). – μ_{eff}(CD$_2$Cl$_2$): 3.1 μ_B. – C$_{90}$H$_{82}$B$_2$Co$_2$F$_8$O$_4$P$_6$ (1705.0): calcd. for **4**·(BF$_4$)$_2$·1 CH$_2$Cl$_2$: C 61.07, H 4.73; found C 60.56, H 5.03.

Table 4. Crystallographic data for **3**·(BF$_4$)$_2$ and **4**·BF$_4$)$_2$

	3·BF$_4$)$_2$	**4**·(BF$_4$)$_2$
formula	C$_{86}$H$_{80}$P$_6$O$_4$Co$_2$B$_2$F$_8$ · 3 (CH$_3$)$_2$CO	C$_{90}$H$_{82}$P$_6$O$_4$Co$_2$B$_2$F$_8$ · 4 CH$_2$Cl$_2$
M_r/g mol^{-1} (without solvates)	1654.9	1705.0
crystal size/mm	0.50 × 0.30 × 0.30	0.40 × 0.30 × 0.20
crystal system	monoclinic	monoclinic
Z	2	2
space group (no.)	$P2_1/c$ (14)	$P2_1/n$ (14)
a/Å	15.794(3)	11.676(4)
b/Å	17.424(3)	13.441(3)
c/Å	18.759(6)	30.421(7)
β [°]	70.42(2)	96.44(3)
V/Å^3	4864(2)	4744(2)
ρ (calcd)/g cm^{-3}	1.249	1.426
T/K	200	200
2θ range [°]	4.5–51.1	3.9–52.0
scan speed/° min^{-1}	$\dot{\omega}$ = 10.0	$\dot{\omega}$ = 10.0
no. rflns measured	9385	9577
no. unique rlfns	9045	9113
no. reflns obs.	6782	5196
obs. criterion	$I > 2\sigma(I)$	$I > 2\sigma(I)$
no. of paramenters	628	581
R_1/%	5.6	8.1
R_w/% (refinement on F^2)	18.2	23.6

[1] O. Kahn, *Angew. Chem.* **1985**, *97*, 837–853; *Angew. Chem. Int. Ed. Engl.* **1985**, *24*, 834–850.
[2] O. Kahn, *Molecular Magnetism*, VCH, Weinheim (Germany), **1993**, and references cited therein.
[3] P. J. Hay, J. C. Thibeault, R. Hoffmann, *J. Am. Chem. Soc.* **1975**, *97*, 4884–4899.
[4] O. Kahn, J. Galy, Y. Journaux, J. Jaud, L. Morgenstern-Badarau, *J. Am. Chem. Soc.* **1982**, *104*, 2165–2176.
[5] Y. Journaux, O. Kahn, H. Coudanne, *Angew. Chem.* **1982**, *94*, 647–648; *Angew. Chem., Int. Ed. Engl.* **1982**, *21*, 624–625.
[6] K.-S. Bürger, P. Chaudhuri, K. Wieghardt, B. Nuber, *Chem. Eur. J.* **1995**, *1*, 583–593.
[7] P. Chaudhuri, K. Oder, K. Wieghardt, S. Gehring, W. Haase, B. Nuber, J. Weiss, *J. Am. Chem. Soc.* **1988**, *110*, 3657–3658.
[8] M. Verdaguer, J. Gouteron, S. Jeannin, Y. Jeannin, O. Kahn, *Inorg. Chem.* **1984**, *23*, 4291–4296.
[9] E. G. Bakalbassis, J. Mrozinsky, C. A. Tsipis, *Inorg. Chem.* **1984**, *23*, 4291–4296.
[10] E. G. Bakalbassis, A: P. Bozopoulos, J. Mrozinsky, P. J. Rentzeperis, C. A. Tsipis, *Inorg. Chem.* **1988**, *27*, 529–532.
[11] Ti^{III}/Ti^{III} dimers: L. C. Francesconi, D. R. Corbin, A. W. Clauss, D. N. Hendrickson, G. D. Stucky, *Inorg. Chem.* **1981**, *20*, 2078–2083.
[12] Fe^{III}/Fe^{III} dimer: M. Dusek, V. Petricek, J. Kamenicek, Z. Sindelar, *Acta Cryst.* **1992**, *C48*, 1579–1582.

[13] E. G. Bakalbassis, C. A. Tsipis, *Inorg. Chem.* **1985**, *24*, 4231−4233.
[14] L. Sacconi, F. Mani, *Transition Met. Chem. (N.Y.)* **1982**, *8*, 179−252, and references cited therein.
[15] R. Morassi, I. Bertini, L. Sacconi, *Coord. Chem. Rev.* **1973**, *11*, 343−402, and references cited therein.
[16] S. Beyreuther, J. Hunger, G. Huttner, S. Mann, L. Zsolnai, *Chem. Ber.* **1996**, *129*, 745−757.
[17] C. Mealli, S. Midollini, L. Sacconi, *Inorg. Chem.* **1975**, *14*, 2513−2521.
[18] C. Furlani, *Coord. Chem. Rev.* **1968**, 3, 141−167, and references cited therein.
[19] B. R. Higginson, C. A. McAuliffe, L. M. Venanzi, *Helv. Chim. Acta* **1975**, *58*, 1261−1271.
[20] For assignments see: J. Ellermann, K. Dorn, *Chem. Ber.* **1966**, *99*, 653−657.
[21] V. Sernau, G. Huttner, J. Scherer, O. Walter, *Chem. Ber.* **1996**, *129*, 243−245.
[22] H. A. Bent, *Chem. Rev.* **1961**, *61*, 275−311.
[23] As the nature of the impurity is not known (presumably oligo- or polymeric species consisting of high-spin Co^{II} and dicarboxylates) the obtained fits to the susceptibilty data are not of the same quality as found with analogous copper compounds.
[24] K. Heinze, S. Mann, G. Huttner, L. Zsolnai, *Chem. Ber.* **1996**, *129*, 1115−1122.
[25] V. Körner, A. Asam, G. Huttner, L. Zsolnai, *Z. Naturforsch.* **1994**, *49b*, 1183−1195.
[26] C. A. Ghilardi, F. Laschi, S. Midollini, A. Orlandini, G. Scapacci, P. Zanello, *J. Chem. Soc. Dalton Trans.* **1995**, 531−540.
[27] V. Körner, G. Huttner, L. Zsolnai, M. Büchner, A. Jacobi, D. Günauer, *Chem. Ber.* **1996**, *129*, 1587−1601.
[28] V. Sernau, G. Huttner, M. Fritz, B. Janssen, M. Büchner, C. Emmerich, O. Walter, L. Zsolnai, D. Günauer, T. Seitz, *Z. Naturforsch.* **1995**, *50b*, 1638−1652.
[29] A. R. Rossi, R. Hoffmann, *Inorg. Chem.* **1975**, *14*, 365−374.
[30] C. Bianchini, D. Masi, C. Mealli, A. Meli, G. Martini, F. Laschi, P. Zanello, *Inorg. Chem.* **1987**, *26*, 3683−3693.
[31] S. Vogel, G. Huttner, L. Zsolnai, *Z. Naturforsch.* **1993**, *48b*, 641−652.
[32] V. Körner, S. Vogel, G. Huttner, L. Zsolnai, O. Walter, *Chem. Ber.* **1996**, *129*, 1107−1113.
[33] K. Heinze, G. Huttner, L. Zsolnai, P. Schober, *Inorg. Chem.* **1997**, *36*, 5457−5469.
[34] A. Weiss, H. Witte, *Magnetochemie*, VCH, Weinheim (Germany), **1973**, 77−94.
[35] [35a] D. F. Evans, *J. Chem. Soc.* **1959**, 2003−2005. − [35b] T. H. Crawford, J. Swanson, *J. Chem. Educ.* **1971**, *48*, 382−386.
[36] A. Muth, *Diplomarbeit*, University of Heidelberg, **1989**.
[37] H. Funk, F. Binder, *Z. Anorg. Allg. Chem.* **1926**, *155*, 327.
[38] [38a] G. M. Sheldrick, *SHELXS 86*, *Program for Crystal Structure Solution*, University of Göttingen, **1986**. − [38b] G. M. Sheldrick, *SHELXL 93*, *Program for Crystal Structure Refinement*, University of Göttingen, **1993**.
[39] L. Zsolnai, G. Huttner, *XPMA*, *ZORTEP*, University of Heidelberg, **1997**.

[97217]